

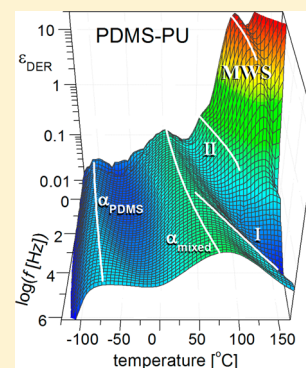
Molecular Dynamics of Segmented Polyurethane Copolymers: Influence of Soft Segment Composition

Daniel Fragiadakis[†] and James Runt^{*,‡}

[†]Naval Research Laboratory, Chemistry Division, Code 6120, Washington, D.C. 20375, United States

[‡]Department of Materials Science and Engineering, Penn State University, University Park, Pennsylvania 16802, United States

ABSTRACT: Dielectric relaxation spectroscopy was used to investigate the molecular dynamics of model segmented polyurethane copolymers having identical hard segments and hard segment weight fractions, but with four different soft segment chemistries of particular interest in biomedical devices. All soft segments have molecular weight ~ 1000 g/mol and are composed of either tetramethylene oxide, hexamethylene oxide, aliphatic carbonate, or dimethylsiloxane (PDMS) segments. These microphase-separated materials exhibit rich dielectric relaxation behavior: up to two relaxations in the glassy state, a segmental α relaxation (two for the polymer with predominately PDMS soft segments), and three slower relaxations. The slowest process arises from interfacial (MWS) polarization, and its strength decreases significantly with increasing temperature (over a few tens of degrees) and disappears at a temperature similar to that at which the small-angle X-ray scattering from the phase-separated microstructure disappears.



INTRODUCTION

For many decades, segmented polyurethane (PU) block copolymers have been used in wide-ranging applications due to their versatile chemistry and relative processing ease. Members of this family of materials are generally synthesized from diisocyanates, short diol chain extenders, and macrodiols having molecular weights up to several 1000 g/mol. Multifunctional reactants can be incorporated when a chemically cross-linked material is desired. The macrodiols serve as the precursors for the PU “soft segments” (amorphous in the unstrained state and having low glass transition temperature (T_g)) while “hard segments” (high T_g and sometimes crystalline) are formed from reaction of the isocyanate-containing molecules and short diols. Because of the random nature of the polymerization, although the soft segments are of fixed length arising from the choice of macrodiol, a broad distribution of hard segment lengths are formed in the polymerization.¹ Because of the significant difference in the chemical nature of hard and soft segments, microphase separation typically occurs on cooling from the melt, resulting in hard and soft domains. PU copolymers with a majority of soft segments in the chains constitute a class of thermoplastic elastomers, with the hard domains serving as the physical cross-links. Hard/soft segment segregation is generally rather incomplete, depending on the specific hard/soft segment chemistry, processing conditions, and other thermal treatments.^{2,3} The nanoscale morphology typically consists of dispersed 3–10 nm scale hard domains³ or in some cases elongated ribbons,⁴ and a soft phase consisting of soft segments and trapped or dissolved (short) hard segments, and interfacial regions.²

Extensive research has been, and continues to be, conducted on new synthesis and exploration of the phase-separated

morphology of segmented polyurethane copolymers, but there has been considerably less work on investigating the molecular dynamics of this family of materials.^{5–8} In a recent paper, we reported the rather rich relaxation behavior of a series of model poly(tetramethylene oxide) [PTMO] soft segment PUs with varying hard segment contents, using dielectric relaxation spectroscopy.⁹ Dielectric spectroscopy is particularly powerful for the investigation of relatively polar polyurethanes, facilitating investigation of the dynamics over a very broad range of frequencies in the glassy and rubbery states. The present paper represents an extension of our earlier study and focuses on model segmented PUs containing ~ 1000 g/mol soft segments, of interest in current blood-contacting biomaterials applications such as cardiac assist devices and pacemaker leads.

EXPERIMENTAL SECTION

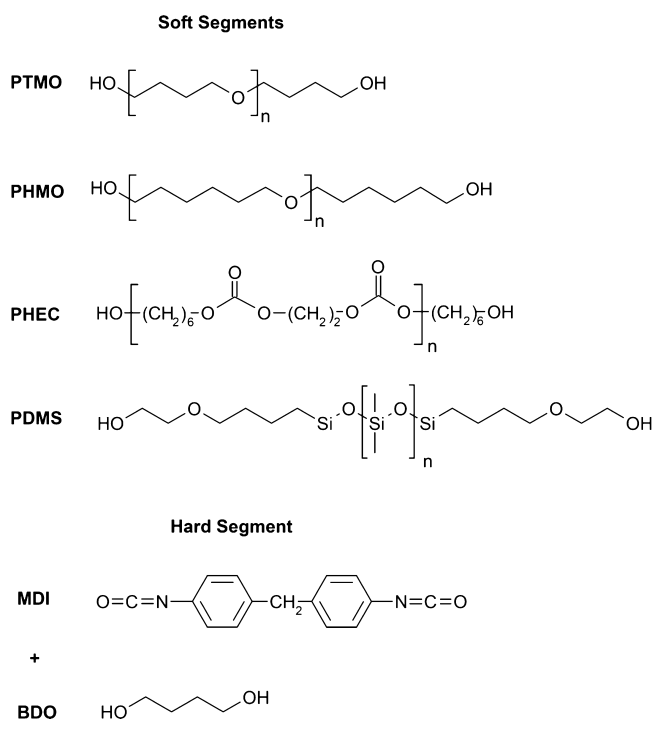
Materials. All four PU copolymers investigated here contain 40 wt % hard segments. The hard segments are composed of 4,4'-methylenediphenyl diisocyanate (MDI) chain extended with 1,4-butanediol (BDO). Various different macrodiols were used to create soft segments (see Scheme 1): a poly(tetramethylene oxide) diol [PTMO], poly(1,6-hexyl 1,2-ethyl carbonate) diol [PHEC], and a poly(hexamethylene oxide) diol [PHMO]. The PTMO and PHEC soft segment precursors have $M_w = 1000$ g/mol, and the PHMO diol has $M_w = 700$ g/mol. A fourth PU copolymer was synthesized using a mixed macrodiol composed of hydroxy-terminated poly-(dimethylsiloxane) (PDMS, $M_w = 1000$ g/mol) and PHMO diol ($M_w = 700$ g/mol), in a ratio of 80/20 w/w. These yielded polyurethanes labeled as PTMO-PU, PHEC-PU, PHMO-PU, and PDMS-PU, respectively. Details of the synthesis and sample

Received: March 27, 2013

Revised: April 25, 2013

Published: May 9, 2013

Scheme 1. Chemical Structures of the Components of the Polyurethanes under Consideration



preparation can be found in ref 3 for PTMO-PU and PHEC-PU, ref 10 for PHMO-PU, and ref 11 for PDMS-PU.

Dielectric Relaxation Spectroscopy (DRS). Samples of 0.1–0.2 mm thickness were sandwiched between 20 mm diameter brass electrodes to form a parallel plate capacitor. Isothermal relaxation spectra were collected under a dry nitrogen atmosphere using a Novocontrol Concept 40 spectrometer from 0.01 Hz to 10 MHz on heating from –120 to 200 °C.

RESULTS AND DISCUSSION

The thermal properties and the microstructure of the PU copolymers under investigation have been extensively characterized in earlier publications^{3,10–12} and are briefly summarized here. In summary, phase-separated hard domains (~5–10 nm in size) were observed for all PU copolymers using tapping mode atomic force microscopy (AFM). AFM phase images also demonstrate that hard domains of each of these copolymers exhibit a noncontinuous morphology of dimension on the order of ~50–75 nm.^{2,3} No hard or soft segment crystallinity was detected for any of the copolymers using wide-angle X-ray diffraction. Degrees of hard/soft segment demixing were quantified by using absolute scattering intensities from small-angle X-ray scattering (SAXS) experiments, primarily using a

general approach originally proposed by Bonart and Mueller.¹³ PTMO-PU, PHMO-PU, and PHEC-PU were found to exhibit a two-phase structure of hard domains dispersed in a soft matrix, with some fraction of the hard segments trapped or dissolved in the soft phase and interfacial regions. PDMS-PU, however, has a unique three-phase core-shell-matrix structure composed of a siloxane matrix, hard domains, and an ether segment-rich mixed phase (the “shell”) surrounding the hard domains.¹⁴ PTMO-PU, PHMO-PU, and PHEC-PU exhibited a single soft phase glass transition, while the PDMS-PU has two, corresponding to the siloxane-rich soft phase and the mixed phase. At higher temperatures, the copolymers exhibit a series of broad complex transitions in differential scanning calorimetry (DSC) thermograms, which correspond to a hard domain glass transition overlapping with hard/soft phase mixing, as confirmed using temperature-resolved synchrotron SAXS.¹² Table 1 summarizes degrees of microphase separation and interdomain spacings from SAXS experiments,³ glass transition temperatures (T_g) and microphase mixing transition temperatures T_{MMT} (defined as the end of the high-temperature DSC endotherm, i.e., the completion of hard domain dissolution in the soft phase) from DSC, and soft phase α transition (from $\tan \delta$ maxima) from dynamic mechanical analysis (DMA) experiments at 1 Hz.^{3,10}

Note that PHEC-PU exhibits considerably greater hard/soft segment mixing compared to the other PUs at room temperature, in keeping with the relatively extensive hydrogen bonding expected between polycarbonate carbonyl and urethane N–H groups in these copolymers.^{3,15} The presence of three phases in the PDMS-PU copolymers precludes quantification of phase separation by the original Bonart–Mueller methodology. However, we demonstrated in an earlier publication that a “pseudo-two-phase” model can be used to analyze the scattering data of PDMS-PU with hard segment contents ≥ 40 wt %.¹⁴ Defined in this way, the degree of phase separation was found to be nearly 1 for the PDMS-PU under consideration here, indicating essentially complete separation of the siloxane segments.

Figure 1 displays complete dielectric spectra of the four polyurethanes investigated, as a function of temperature and frequency, in the so-called derivative representation:¹⁶

$$\epsilon_D = -\frac{\pi}{2} \frac{d\epsilon'}{d \ln \omega}$$

The derivative has the same features as the loss spectrum but is free of dc conduction losses that often obscure low-frequency relaxation processes. For relatively broad peaks, ϵ_D is a good approximation of the dielectric loss, whereas more narrow peaks are significantly narrower in ϵ_D than in ϵ'' , helping to resolve overlapping processes. This is illustrated for a

Table 1. Degree of Microphase Separation and Interdomain Spacing from SAXS,³ Microphase Mixing Temperature estimated from the end of the high- T DSC endotherm^{3,10} and from the temperature at which the MWS process disappears, and Soft Phase Glass Transition Temperatures from DSC and/or the Soft Phase T_α Transition from DMA,^{3,10} the latter in parentheses, and dielectric measurements (defined as $\tau_\alpha(T_{g,die}) = 1/2\pi f_{max,\alpha}(T_{g,die}) = 100$ s)

	degree of microphase separation	interdomain spacing [nm]	T_{MM} [°C] from DSC	T_{MM} [°C] from DRS	T_g [°C] from DSC (T_α from DMA)	$T_{g,die}$ [°C]
PTMO-PU	0.29	13.0	175	153	–50	–45
PHMO-PU	0.34	11.4	160	149	–21	–19
PHEC-PU	0.13	13.0	155	146	–15 (9)	–10
PDMS-PU	~1	8.9	180	153	(–95) (25)	–110, –6

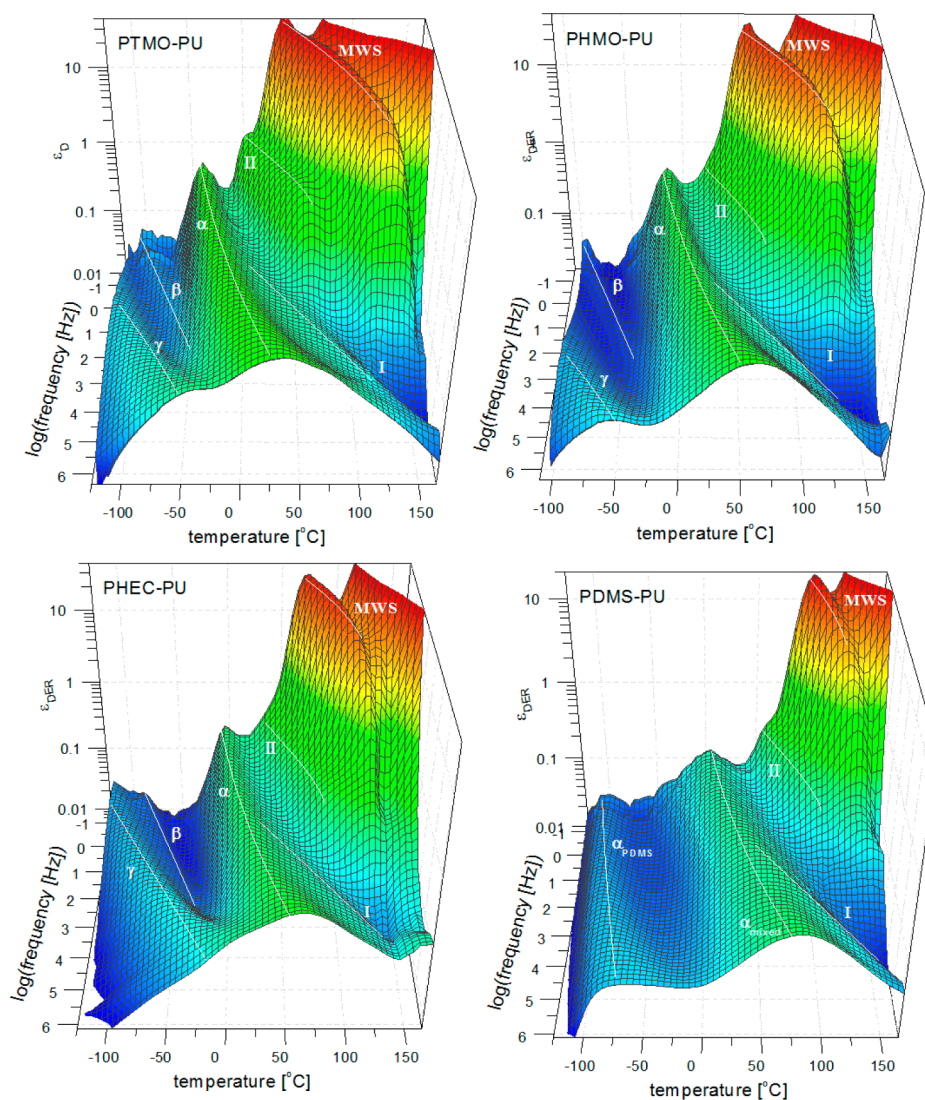


Figure 1. Conductivity-free dielectric relaxation spectra (using the derivative representation) as a function of frequency and temperature for the polyurethanes under consideration.

representative case (PTMO-PU) in Figure 2: at high temperatures the dc conductivity obscures three low-frequency relaxation processes; however, these are visible in the real part ϵ' of the dielectric function and therefore also in ϵ_D .

All four polyurethanes exhibit rich relaxation behavior. PTMO-PU, PHMO-PU, and PHEC-PU exhibit two relaxations in the glassy state (β and γ), a soft phase segmental α relaxation, and three slower relaxations which we have labeled I, II, and MWS. PDMS-PU, having a three-phase core-shell structure and two soft glass transitions, also exhibits two α relaxations, a single weak secondary β process, and the high-temperature I, II, and MWS peaks.

The derivative and dielectric loss spectra were fit using a sum of the appropriate form of the Havriliak-Negami function for each relaxation peak:¹⁷

$$\epsilon^*(f) = \frac{\Delta\epsilon}{[1 + (if/f_{HN})^a]^b}$$

where $\Delta\epsilon$ is the dielectric increment (contribution to the static dielectric constant), a and b are shape parameters with $0 < a$ and $ab \leq 1$, and f_{HN} is a characteristic frequency related to the frequency of maximum loss, f_{max} by

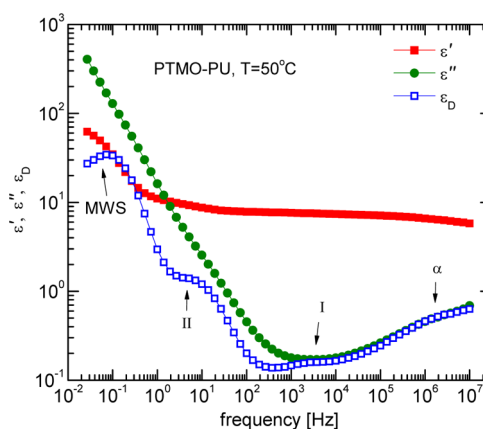


Figure 2. Representative dielectric spectrum for the polyurethanes above the glass transition: Real and imaginary parts of the dielectric permittivity and derivative ϵ_D . The I, II, and MWS processes are clearly visible in ϵ' and ϵ_D but obscured by dc conductivity in the dielectric loss.

$$f_{\max} = f_{\text{HN}} \left[\frac{\sin\left(\frac{\pi a}{2+2b}\right)}{\sin\left(\frac{\pi ab}{2+2b}\right)} \right]^{1/a}$$

Additionally, some values of f_{\max} were read directly from the maximum of isochronal plots of ϵ'' or ϵ_D (data at a fixed frequency as a function of temperature).

The resulting relaxation frequencies are plotted as a function of inverse temperature in Figure 3. Their temperature

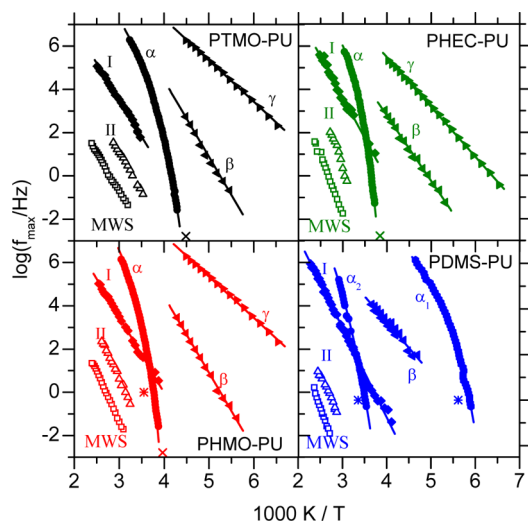


Figure 3. Dielectric relaxation frequencies as a function of inverse temperature for the four polyurethanes. Lines are fits to the Arrhenius and VTF equations. The α relaxation temperatures from dynamic mechanical analysis (*, at 1 Hz) and calorimetric glass transition temperatures (X, at an equivalent relaxation time of 100 s) are also included.

dependence was fit using the Vogel–Tammann–Fulcher (VTF) equation

$$f_{\max} = f_0 \exp\left(-\frac{B}{T - T_0}\right)$$

for the α relaxations, where f_0 , B , and T_0 (Vogel temperature) are temperature-independent empirical parameters and the Arrhenius equation

$$f_{\max} = f_0 \exp\left(-\frac{E_a}{kT}\right)$$

for the β , γ , and I relaxations, where E_a is the activation energy. The fit parameters are shown in Table 2. In the following we examine each relaxation process in detail.

Glassy State Motions. PTMO–PU and PHMO–PU have two secondary relaxations, β and γ . The γ process is attributed

to local chain motions, specifically crankshaft motions of the ether oxygen containing segments.¹⁸ This is supported by the identical temperature dependence in the two materials. The weaker, slower β process is present in a wide variety of water-containing systems and has been associated with reorientational motions of water molecules.^{19–21} PHEC–PU exhibits two secondary relaxations, β and γ . The assignment of these processes remains unclear, but they are associated with local motions of main chain and/or carbonate group in the soft PHEC phase, possibly also (in the case of β) with some contribution from water molecules.

PDMS–PU has a weak secondary relaxation in the temperature range between the two segmental processes. In this temperature range the siloxane phase is well above its glass transition; therefore, we associate this β process with local motions in the glassy mixed phase. However, given the complex chemical nature of this phase, we cannot at this stage make a more specific assignment.

Segmental Relaxation. PTMO–PU, PHMO–PU, and PHEC–PU each exhibit a single α relaxation process, corresponding to segmental motions in the soft phase. The temperature at which the extrapolated relaxation time is $\tau_\alpha = 100$ s is in good agreement with the calorimetric glass transition temperature (see Table 1). As is usual for segmental relaxations in amorphous polymers, and was observed previously for PTMO-based polyurethanes,⁹ the relaxation strength $\Delta\epsilon_\alpha$ decreases with increasing temperature.

The dielectric spectrum of PDMS–PU displays two α relaxations: the faster α_1 related to the dynamics of the soft PDMS phase and the slower α_2 corresponding to segmental dynamics in the mixed phase (“shell” in the core–shell structure). Two segmental relaxations were observed for these materials previously using dynamic mechanical analysis.^{3,14} Peak temperatures of the mechanical $\tan \delta$ spectra are included in Figure 3 (denoted by asterisks on the plots at 1 Hz) and are consistent with the dielectric data (given that relaxation times from mechanical data are typically shorter than dielectric relaxation times²²).

Process I. In all four polyurethanes, process I appears at high temperatures as a low-frequency shoulder on the α process (on α_2 for PDMS–PU). At lower temperatures, as its relaxation time is less sensitive to temperature than the segmental relaxation time, it overlaps and eventually becomes slower than the α relaxation (see Figure 4). This is seen most clearly for PDMS–PU. The temperature dependence of its maximum loss frequency is well described by the Arrhenius equation with a rather large activation energy of 0.66–0.78 eV. The strength $\Delta\epsilon_I$ of this process decreases with increasing temperature (see Figure 5). It is striking that the relaxation time and its temperature dependence for process I change little with soft segment chemistry, even though the soft phase α relaxation times vary by many orders of magnitude and their temperature

Table 2. Activation Parameters for the α , β , γ , and I Processes^a

	γ		β		α			I	
	$\log(f_0/\text{Hz})$	E_a [eV]	$\log(f_0/\text{Hz})$	E_a [eV]	$\log(f_0/\text{Hz})$	B [K]	T_0 [K]	$\log f_0$	E_a [eV]
PTMO–PU	14.9	0.38	19.0	0.72	11.8	1623	180	13.5	0.66
PHMO–PU	14.8	0.37	18.5	0.70	12.0	1649	206	13.9	0.69
PHEC–PU	14.7	0.46	14.8	0.59	10.9	1210	225	15.2	0.76
PDMS–PU			12.5	0.45	10.0, 14.0	666, 3208	141, 184	15.1	0.78

^aPDMS–PU has two α processes corresponding to the soft and mixed phases and has no γ process.

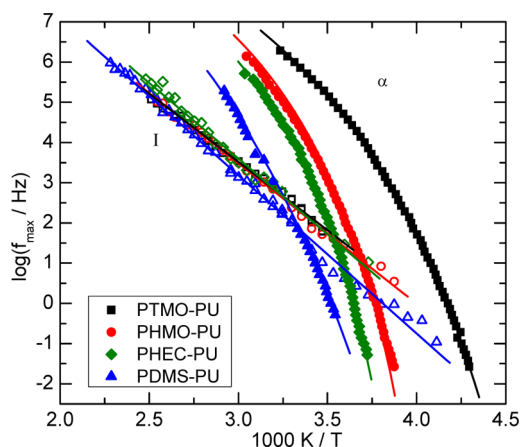


Figure 4. Dielectric relaxation frequencies for process I and the soft phase α relaxation (mixed phase α_2 for PDMS-PU). Process I occurs in the same frequency range and with similar activation energies for all PUs, despite the widely different segmental dynamics.

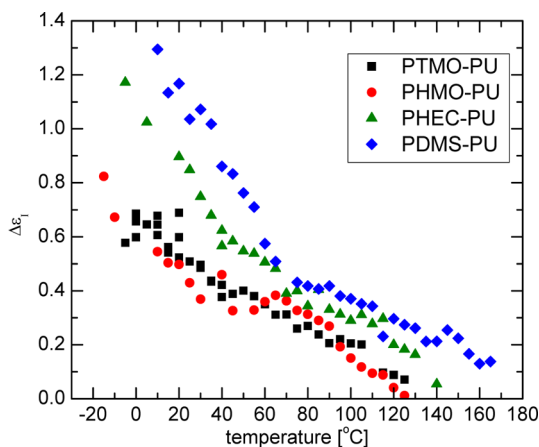


Figure 5. Strengths of process I as a function of temperature for the four polyurethanes.

dependence is very different. Clearly, process I is not coupled to the soft phase segmental motions (or to the mixed phase, in the case of PDMS-PU). Also, in PTMO-based polyurethanes, the intensity of process I was found to systematically increase with hard segment content.⁹

This process has been observed in previous studies of PTMO-MDI based polyurethanes and has been attributed to segmental motion in the interfacial regions close to the hard domains,^{23,24} or to crystallization of (higher MW) PTMO chain segments.⁶ The former explanation would account for the dependence of $\Delta\epsilon_1$ on hard segment content and on temperature. However, this interpretation can be ruled out by the lack of any correlation between the time scales of the segmental and I processes. No crystallization is observed in the soft segments of any of the four polyurethanes. Process I also is unlikely to originate in interfacial polarization, since its temperature dependence is not correlated with dc conductivity.

It is reasonable therefore to attribute process I to molecular motions in the hard domains, which would explain the relative insensitivity to soft phase chemistry, and the relaxation strength dependence on hard segment content. It cannot be the segmental process of the hard phase: extrapolating $\tau_1 = 100$ s would give a “glass transition temperature” of -60 ± 10 °C, very far from the hard segment T_g of ~ 60 °C suggested by DSC

measurements.³ Given also its Arrhenius temperature dependence, we speculate that process I originates in local motions of strongly hydrogen-bonded segments in hard domains. The decrease of its relaxation strength on heating is opposite of what is typically observed for secondary relaxation processes. However, this behavior is consistent with our hypothesis for the origin of process I if, as hydrogen bonds between hard segments progressively break with increasing temperature, these loosely bonded segments no longer contribute to process I. Eventually at higher temperatures, the hard domains gradually dissolve in the soft matrix,¹² and the intensity of process I becomes zero.

Process II. Process II is observed in all four polyurethanes, at lower frequencies than process I. The relaxation time and its temperature dependence are different for each soft segment chemistry, unlike process I. The hard segment α relaxation might be expected in this temperature range. Figure 6 shows

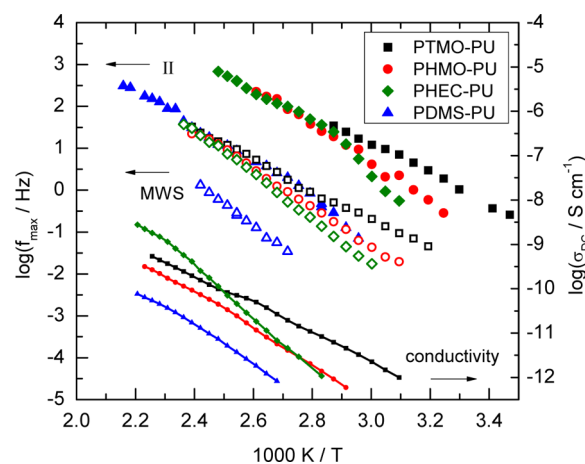


Figure 6. Relaxation frequencies of process II and the MWS process along with dc conductivity.

the relaxation frequencies for process II and the interfacial MWS relaxation, along with the dc conductivity for all four polyurethanes. The relaxation time of process II is clearly correlated to the dc conductivity of the soft phase. It is more likely, therefore, that process II is related to charge carrier mobility in the soft phase. As can be seen in Figure 2, its frequency is close to the point where $\epsilon' = \epsilon''$; this is the frequency range where additional peaks due to dielectric inhomogeneities usually occur.²⁵ However, it is not clear what these inhomogeneities are; process II is distinct from the slower and more intense MWS peak discussed in the next section, which corresponds to interfacial polarization at the hard-soft domain boundaries.

Interfacial Polarization. In heterogeneous materials with regions having different dielectric permittivity or conductivity, interfacial polarization occurs due to accumulation of charges at the interfaces. The accumulating charges behave similarly to a macroscopic dipole, giving rise to a dielectric loss peak (Maxwell-Wagner-Sillars (MWS) polarization).^{26,27} The MWS process appears in the frequency range of the loss dominated by dc conductivity of ionic impurities in the soft phase. Representative dielectric spectra are shown in Figure 7. The frequency and intensity of the MWS process depend on the dielectric “contrast” between the soft matrix and hard domains, i.e., the difference between their respective dielectric constants and conductivities. At low temperatures, $\Delta\epsilon_{MWS}$

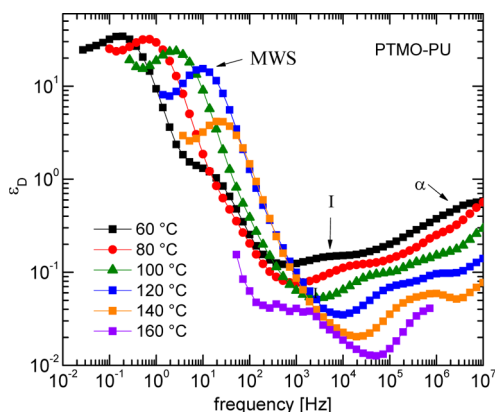


Figure 7. Representative dielectric spectra in the region of the MWS process for PTMO-PU. The intensity of the MWS process decreases sharply beginning at 120 °C.

exhibits large values (~ 25 for PDMS-PU, 50–100 for the other PUs), which are in the usual range for interfacial polarization of multiphase polymer systems.²⁷ On heating, $\Delta\epsilon_{\text{MWS}}$ slightly increases or remains approximately constant for several tens of degrees and then decreases relatively rapidly and approaches zero at $T > 150$ °C.

We have found previously, using temperature-dependent synchrotron small-angle X-ray scattering, that these polyurethanes undergo phase mixing at elevated temperatures, signaled by a decrease in scattered intensity and finally the disappearance of the small-angle scattering peak.¹² This is a gradual process, taking place over a few tens of degrees. A complex and broad endotherm is also observed in DSC measurements in the same temperature range, associated with phase mixing.^{3,12} In Figure 8 we plot $\Delta\epsilon_{\text{MWS}}$ along with the total scattered intensity from SAXS. The phase mixing temperatures corresponding to the end of the DSC endotherm are also indicated on the plot. The temperature dependence of $\Delta\epsilon_{\text{MWS}}$ mirrors qualitatively the behavior of the total scattered intensity Q . However, the drop in Q is more gradual and at

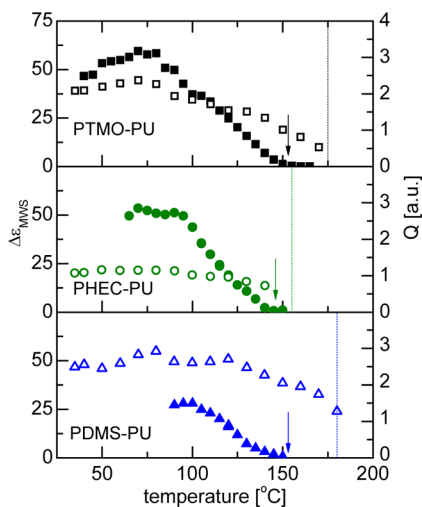


Figure 8. Intensity of the MWS process (filled symbols) and total scattered intensity from SAXS (open symbols) as a function of temperature. The arrows indicate the temperature where $\Delta\epsilon_{\text{MWS}}$ becomes approximately zero; the dashed vertical lines are the microphase mixing temperatures estimated from DSC measurements.

higher temperatures. This discrepancy can be ascribed to a kinetic effect: dielectric spectroscopy was conducted using stepwise 5 °C temperature changes followed by ~ 1 h waiting time for temperature stabilization and measurement at each temperature, while DSC and SAXS were conducted at a constant heating rate of 10°/min. The difference between T_{MMT} obtained at a faster rate (SAXS and DSC, in agreement with each other) vs a much slower rate (DRS) gives a qualitative measure of the kinetics of phase mixing: a larger difference between the two temperatures corresponds to faster kinetics of phase mixing. Therefore, the results of Figure 8 indicate that at a given temperature phase mixing proceeds increasingly rapidly in the order PHEC-PU, PTMO-PU, PDMS-PU. This is the order of decreasing soft-segment T_g , as we would expect if the kinetics of phase mixing is strongly influenced by the segmental dynamics of the soft phase. It is also the order of decreasing soft-hard segment compatibility and (initial) degree of phase separation. Therefore, one would expect that the thermodynamic driving force for phase mixing becomes weaker going from PHEC to PTMO to PDMS, and the initial structure is increasingly phase separated; however, phase mixing occurs faster at a given temperature, presumably because of more rapid segmental dynamics.

SUMMARY

Dielectric spectra of microphase-separated PUs exhibit a variety of relaxations in the glassy and rubbery states. One of the keys to successfully interpreting PU dielectric spectra (indeed, for all phase-separated materials) is knowledge of the details of the microphase-separated structure. Such characterization on the four model PUs (having identical thermal history as those studied herein) is described in refs 3, 10, 11, and 12.

PTMO-PU, PHMO-PU, and PHEC-PU exhibit two glassy state processes. For the former two copolymers, the lowest temperature (γ) process is attributed to local crankshaft-type motions of ether oxygen containing segments. These copolymers exhibit a weak, slower β process, which we associate with motions of water molecules (even though the samples were extensively dried prior to dielectric measurements). PHEC-PU also exhibits two secondary relaxations and are likely associated with local motions of the main chain and/or carbonate groups in the PHEC-rich phase, possibly along with some contribution from water molecules. The dielectric spectrum of PDMS-PU has one weak secondary relaxation in the temperature range between its two segmental processes, which we associate with local motions in the glassy mixed phase of this copolymer.

As expected, PTMO-PU, PHMO-PU, and PHEC-PU exhibit a single α relaxation, whose extrapolated relaxation time (to $\tau_\alpha = 100$ s) is in good agreement with the DSC T_g of each copolymer. The dielectric spectrum of PDMS-PU displays two α relaxations: the faster α_1 process is assigned to the segmental dynamics of the PDMS phase, and the slower α_2 relaxation is associated with segmental dynamics in the mixed phase (“shell”) of this unique three-phase PU.

Removing the contribution of dc loss from loss spectra facilitates observation of three higher temperature processes in all copolymers under investigation, which we refer to as the I, II, and MWS processes. The relaxation times and temperature dependence of process I varies little with soft segment chemistry, exhibits Arrhenius behavior with relatively large activation energy (0.66–0.78 eV), and the relaxation strength was found in our previous study of PTMO-PUs to increase

systematically with hard segment content.⁹ Considering the available information, we propose that process I originates in local motions of strongly hydrogen-bonded segments in hard domains.

The MWS process appears in the frequency range dominated by dc conductivity in the soft phase. On heating, the relaxation strength decreases significantly (over a range of tens of degrees) and approaches zero at elevated temperatures. Although the disappearance of the MWS process qualitatively correlates with changes in the small-angle X-ray scattering invariant with increasing temperature, the invariant changes more slowly and the disappearance of the X-ray scattering associated with the microphase-separated structure (and T_{MMT} estimated from DSC experiments) occurs at a higher temperature than the disappearance of the MWS relaxation. We propose that these differences arise because of kinetic effects: the difference between T_{MMT} obtained at a faster rate (SAXS and DSC, in agreement with each other) vs a much slower rate (dielectric spectroscopy) provides a (qualitative) measure of the kinetics of hard–soft phase mixing, with a larger difference between the two temperatures corresponding to more rapid mixing. Our findings indicate that phase mixing proceeds increasingly rapidly in the order PHEC–PU, PTMO–PU, to PDMS–PU, presumably due to more rapid segmental dynamics.

AUTHOR INFORMATION

Corresponding Author

*E-mail runt@matse.psu.edu.

Notes

The authors declare no competing financial interest.

ACKNOWLEDGMENTS

The authors express their appreciation to the National Science Foundation, Polymers Program, for support of this research under Grants DMR-0907139 and DMR-1206571. This work was supported in part by the Office of Naval Research. We also thank AorTech Biomaterials (Dr. Ajay Padsalgikar and Ms. Jadwiga Weksler) for providing the PUs used in this investigation.

REFERENCES

- (1) Peebles, L. H. *Macromolecules* **1976**, *9*, 58.
- (2) Koberstein, J. T.; Stein, R. S. *J. Polym. Sci., Polym. Phys.* **1983**, *21*, 1439.
- (3) Hernandez, R.; Weksler, J.; Padsalgikar, A.; Choi, T.; Angelo, E.; Lin, J. S.; Xu, L.-C.; Siedlecki, C. A.; Runt, J. *Macromolecules* **2008**, *41*, 9767.
- (4) Klinedinst, D. B.; Yilgör, I.; Yilgör, E.; Zhang, M. Q.; Wilkes, G. L. *Polymer* **2012**, *53*, 5358.
- (5) Pissis, P.; Georgoussis, G.; Bershtein, V. A.; Neagu, E.; Fainleib, A. M. *J. Non-Cryst. Solids* **2002**, *305*, 150.
- (6) Czech, P.; Okrasa, L.; Mechin, F.; Boiteux, G.; Ulanski, J. *Polymer* **2006**, *47*, 7207.
- (7) Okrasa, L.; Czech, P.; Boiteux, G.; Mechin, F.; Ulanski, J. *Polymer* **2008**, *49*, 2662.
- (8) Polizos, G.; Kyritsis, A.; Pissis, P.; Shilov, V. V.; Shevchenko, V. V. *Solid State Ionics* **2000**, *136*, 1139.
- (9) Castagna, A. M.; Fragiadakis, D.; Lee, H.-K.; Choi, T.; Runt, J. *Macromolecules* **2011**, *44*, 7831.
- (10) Choi, T.; Weksler, J.; Padsalgikar, A.; Runt, J. *Polymer* **2009**, *50*, 2320.
- (11) Choi, T.; Weksler, J.; Padsalgikar, A.; Runt, J. *Polymer* **2010**, *51*, 4375.

(12) Pongkitwittoon, S.; Hernandez, R.; Weksler, J.; Padsalgikar, A.; Choi, T.; Runt, J. *Polymer* **2009**, *50*, 6305.

(13) Bonart, R.; Mueller, E. H. *J. Macromol. Sci., Phys.* **1974**, *B 10*, 345.

(14) Hernandez, R.; Weksler, J.; Padsalgikar, A.; Runt, J. *Macromolecules* **2007**, *40*, 5441.

(15) Gunatillake, P. A.; Meijs, G. F.; McCarthy, S. J.; Adhikari, R.; Sherriff, N. *J. Appl. Polym. Sci.* **1998**, *69*, 1621.

(16) Wübbenhorst, M.; van Turnhout, J. J. *Non-Cryst. Solids* **2002**, *305*, 40.

(17) Havriliak, S.; Negami, S. *J. Polym. Sci., Polym. Symp.* **1966**, *14*, 99.

(18) Hedvig, P. *Dielectric Spectroscopy of Polymers*; Adam Hilger: Bristol, 1977.

(19) Cervený, S.; Alegría, A.; Colmenero, J. *Phys. Rev. E* **2008**, *77*, 031803.

(20) Capaccioli, S.; Ngai, K. L.; Shinyashiki, N. *J. Phys. Chem. B* **2007**, *111*, 8197.

(21) Fragiadakis, D.; Runt, J. *Macromolecules* **2010**, *43*, 1028.

(22) McCrum, N. G.; Read, B. E.; Williams, G. *Anelastic and Dielectric Effects in Polymeric Solids*; Dover Publications: New York, 1991.

(23) Raftopoulos, K. N.; Pandis, C.; Apekis, L.; Pissis, P.; Janowski, B.; Pielichowski, K.; Jaczewska, J. *Polymer* **2010**, *51*, 709.

(24) Raftopoulos, K. N.; Janowski, B.; Apekis, L.; Pielichowski, K.; Pissis, P. *Eur. Polym. J.* **2011**, *47*, 2120.

(25) Richert, R.; Agapov, A.; Sokolov, A. P. *J. Chem. Phys.* **2011**, *134*, 104508.

(26) van Beek, L. K. H. *Dielectric Behavior of Heterogeneous Systems*; Heywood Books: London, 1967.

(27) North, A. M.; Petrick, R. A.; Wilson, A. D. *Polymer* **1978**, *19*, 923.